

0017-9310(94)00116-2

# The jet mixing effect on reaction flow in a bluff-body burner

H. K. MA and J. S. HARN

Department of Mechanical Engineering, National Taiwan University, Taipei, Taiwan, R.O.C.

(Received 12 February 1994)

**Abstract**—This study investigates the mixing effects of primary and secondary jets on flame stability as fuel/air is injected into a bluff-body burner. A two-dimensional spray combustion model, based upon a SIMPLER method, is used for numerical studies of combusting flow. The influence of the jet-to-air velocity ratio on the recirculation zone behind the bluff body, the center axial velocity and the temperature profiles is studied in detail. The results show that mixing between the two jets is controlled by two vortex eddies on the inside and outside of the bluff-body. With a proper bluff-body blockage ratio, cone angle and jet-to-air velocity ratio a more stable flame can be achieved.

## INTRODUCTION

Bluff-body burners are widely used in gas turbine combustors to achieve better mixing of fuel and air, better flame stability and less emission of pollutants. The flow field for the bluff-body burner in a combustion chamber primarily consists of the principal circulation zone created by the primary and secondary jets, the recirculation zone behind the bluff body, and the outer recirculation zone formed by the projecting walls. This recirculation zone forms a low-velocity zone with a longer residence time, in which the ignition source may linger and deliver the flame to the unburned mixture, generating a more stable flame.

Hedley and Jackson [1] found that recirculation was helpful in mixing fuel and air. This finding led to attention being given to the formation of the recirculation zone in a combustion system. Wingfield [2] conducted a simulated experiment on a double concentric jet under a cold flow. He concluded that the greatest mixing of the primary and secondary jets occurred when the bluff-body thickness ratio ( $d_2/d_1$ ) was between 2 and 3; and that the intensity of the primary fuel jet decreased when the velocity ratio ( $U_s/U_p$ ) and momentum ratio ( $G_s/G_p$ ) increased. Focusing on the variations in the double concentric jet in a combustion chamber with a cold flow, Habib and Whitelaw [3] found that the length and velocity ratio of the outer corner recirculation zone were related to the geometric shape of the combustion chamber, and that the greater the velocity ratio, the greater the velocity gradient in the mixed zone. Smith *et al.* [4] examined the distribution of the static pressure, total stress, and velocity on the combustion chamber walls. They discovered that a chemical reaction could change the size and position of the recirculation zone, and that the static pressure distributions of both the combustion and cold flow were uneven. In the combustion flow, the static pressure

increased, the total stress decreased, and the decline in the intensity and velocity slowed down due to a combustion reaction.

Schefer *et al.* [5] classified flames into two types of jet that control the circulation field, air-flow or fuel-flow, which were determined by the velocity ratio between the primary fuel jet and the surrounding, secondary air jet. They found that the secondary air jet tended to wrap around the central axis and form a tail circulation zone, and the secondary air jet and center primary fuel jet act on each other in the main circulation zone. Under non-combustion circumstances, there are obviously two stagnation points on the central axis line, which are, respectively, formed by the primary fuel jet and the surrounding secondary air jet. However, only one stagnation point exists on the central axis. The reason for this lies in the fact that, during combustion, the gas volume expands, and the density decreases, which increases the penetration of the fuel jet. This leads to the stagnation point of the fuel jet moving substantially downstream. On the contrary, the stagnation point of the air jet is not affected much by combustion. Therefore, the air and fuel stagnation points overlap. However, the total volume of the recirculation zone remains constant. This is different from another situation in which the recirculation zone increases considerably due to the expansion of burning air in the burning premixing flame.

Chen *et al.* [6] compared the effects of a bluff body and an eddy on flame stability. They presented two important parameters affecting the flame type: (1) eddy vortex circulation, and (2) jet momentum. Both the central bluff body and eddy circulation can produce a large area of recirculation whose front stagnation point position is an important factor in determining flame stability and the delivery of energy to the nozzle. An improvement in the mixing of fuel and air can shorten the flame length considerably. As for

## NOMENCLATURE

<b>BR</b>	blockage ratio, $(d_2/d_s)^2$	$U_s$	secondary-jet velocity
$d$	diameter	$U_p/U_s$	jet-to-air velocity ratio.
$D_c$	diameter of combustion chamber	Greek symbols	
<b>ER</b>	expansion ratio, $d_s/D_c$	$\alpha$	cone angle
$f$	flow flux	$\varepsilon$	turbulence dissipation rate
$G$	momentum flux	$\xi$	flow variable
$h$	total enthalpy	$\phi$	mixture fraction.
$K$	turbulent kinetic energy	Subscripts	
$L_{rz}$	length of recirculation zone	cen	center
$P_o$	static pressure of entrance wall	f	fuel
$P_w$	wall static pressure	g	gas
$Re$	Reynolds number	o	single jet
$R_c$	radius of combustion chamber	p	primary jet
$S$	stoichiometric oxygen/fuel ratio,	s	secondary jet
	source term	0	initial or inlet condition.
$U$	mean velocity		
$U_p$	primary-jet velocity		

the effects of the recirculation field near the nozzle on the flame persistence and stability, Pan *et al.* [7] proposed five important parameters which might affect flame persistence: (1) the blockage ratio of the bluff body, (2) the cone angle (2) of the bluff body, (3) the velocity of the incoming mixture, (4) the turbulence intensity, and (5) the mixture equivalence ratio of the experiment. During burning, the recirculation zone behind the bluff body increases due to air expansion resulting from burning, and the structure of the flow field also changes. Pan *et al.* [8] studied the nature of the turbulence of a cone-shaped flame in a closed circulation field, and measured the turbulence movement, the Reynolds shear stress, the average axial stress gradient, and the structure of the recirculation zone. They found that the recirculation zone size decreased when the blockage ratio or turbulence intensity of the combustion flow increased. When the cone angle of the bluff body increased, the volume of the recirculation zone increased slightly. As the mixture equivalence ratio increased, the length of the recirculation zone decreased. When the turbulence intensity increased, the length of the recirculation zone distinctly decreased, whose value was close to that in an isothermal flow field.

Namazian *et al.* [9] studied several isothermal conditions. They concluded that the jet-to-air velocity ratio, or momentum-flux ratio, is an important parameter in fuel and air mixing. The jet penetrates the recirculation zone formed behind the bluff body for momentum-flux ratios  $< 1$ . For momentum-flux ratios  $> 1$ , the fuel jet stagnates and does not penetrate the recirculation zone, and fuel is dispersed into the recirculation zone. This momentum-flux ratio also governs the fuel concentration inside the recirculation zone. For low momentum-flux ratios, considerable portions of the field are mixed under conditions where

combustion could occur. The region could occupy a much greater portion of the field than those for free-jet flames with no bluff body present. This enhanced mixing is the reason for sustaining a more stable flame with the bluff-body burner. Penetrated-jet cases show increased mixing relative to a free jet. Inside the recirculation zone the flow is similar to a free jet.

Martins and Ghoniem [10] focused on the time-dependent dynamics and the effect of the diameter ratio across the bluff body on the wake flow. They found that shedding is inhibited if the inner-jet velocity is much smaller than the annular-flow velocity. The stabilization of the recirculation zone due to the presence of the inner jet is associated with the formation of large eddies as the vorticity carried by the jet fluid rolls downstream of the bluff body. Shedding results from the competition between the annular-flow eddy and the jet eddy as they compete to attach to the bluff-body face. The mixing between the two flows is governed by the merging of eddies forming on the inner and outer edges of the bluff body and the formation of structures at the downstream end of the wake. When the flow is jet-dominated the jet penetrates the recirculation zone and enters the annular fluid as it leaves the region while the average stagnation point is off-axis. The entrainment mechanism is the merging of the two eddies. The fluctuation level increases and the frequency of shedding decreases as the diameter ratio increases. Also, the average length of the overall recirculation bubble is almost 1.5 times the diameter of the bluff body.

Ma *et al.* [11, 12] investigated spray flow in a gas turbine combustor by a SIMPLER method. They found that the reaction flow will have a shorter recirculation zone than the isothermal flow. The length of the recirculation zone at the corner (or behind the bluff body) is linearly proportional to the expansion

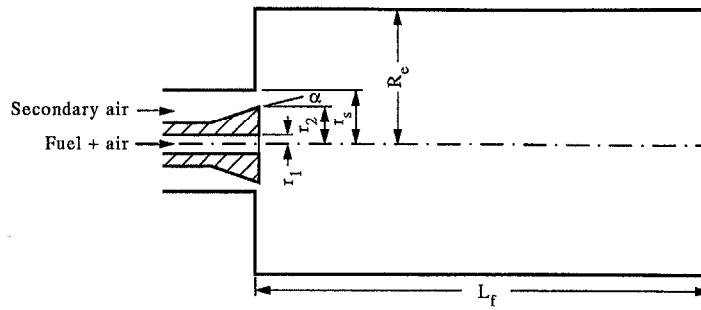


Fig. 1. Schematic of combustor with a bluff body.

ratio (or bluff-body ratio). In comparison with reaction flow and isothermal flow, the slope ratio is 0.43 for the recirculation zone at the corner and 0.48 for the recirculation zone after the bluff body.

In general, a bluff-body burner may provide a fuel-rich mixture near a nozzle, and a fuel-lean mixture further downstream. Therefore, the geometric shape of the bluff-body combustor and the jet mixing affecting the combustion process (especially flame stability) are closely related to the aerodynamics of the circulation field. In particular, the structure of the circulation zone, and the positions of the front and back stagnation points are very helpful for understanding the process of flame stability.

#### NUMERICAL FORMULATION AND NUMERICAL METHOD

A cylindrical spray combustion chamber equipped with a bluff-body combustor was used in this study (cf. Fig. 1). The normalized conservation equations for the gas phase variables and the droplet number densities are written in the general form as

$$\frac{1}{r} \left[ \frac{\partial}{\partial x} \left( r f_x \xi - r y \frac{\partial \xi}{\partial x} \right) + \frac{\partial}{\partial r} \left( r f_r \xi - r y \frac{\partial \xi}{\partial r} \right) \right] = S_{\xi_1} + S_{\xi_2}. \quad (1)$$

The normalized concentration equations for the droplet variables and temperature are written as

$$\frac{1}{r} \left[ \frac{\partial}{\partial x} \left( r f_x \xi + \frac{\partial}{\partial r} (r f_r \xi) \right) - \frac{\xi}{r} \left[ \frac{\partial}{\partial x} (r f_x) + \frac{\partial}{\partial r} (r f_r) \right] \right] = S_{\xi_2}. \quad (2)$$

$S_{\xi_1}$  and  $S_{\xi_2}$  are the intra- and interphase terms, respectively. The initial and boundary conditions are as follows:

Entrance:

$$\frac{U_g}{U_{go2}} = (1-r)^{1/7}; \quad V_g = 0$$

$$K_{in} = 0.005(U_{go2})^2$$

$$\varepsilon_{in} = C_{\mu} \cdot K^{3/2} / (0.03 R_c).$$

Exit:

$$\frac{\partial u}{\partial x} = 0; \quad v = 0; \quad \frac{\partial \xi}{\partial x} = 0$$

where  $\xi = k, \varepsilon, h, \phi, v_{d,k}, n_{d,k}$ .

Impermeable wall:

$$\left( \frac{\partial \xi}{\partial r} \right)_{wall} = 0 \text{ (except } \xi = U_g)$$

$$(U_g)_{wall} = (V_g)_{wall} = 0.$$

Axisymmetric axis:

$$\left( \frac{\partial \xi}{\partial r} \right)_{axis} = 0; \quad V_g = 0.$$

The generalized forms of the elliptic partial differential equations are separated into approximate algebraic forms by integrating them over the computational cells within the combustor. A staggered grid system is adopted with all scalar quantities evaluated at the nodal points of the cells, and gas velocity components evaluated at the cell faces. For the calculation of fluxes across the boundary faces a special treatment is adopted along the boundaries. Infinitely thin control volumes are introduced to establish the conservation of fluxes on the boundaries. The wall functions are used for the near-wall regions to bridge the regions where the effect of the molecular viscosity dominates the near wall.

A two-dimensional spray combustion code [11, 12], based upon the SIMPLER procedure, is employed to solve for the gas phase flow and gas-liquid flow field. A power law scheme is used to calculate the combined convection/diffusion fluxes through the interfaces of the control volumes whereas an upwind scheme is used to calculate the fluxes in the flow field, and the line-by-line TDMA method is adopted to solve the algebraic equation.

Ma *et al.* [12] used the above numerical method in studying heat and mass transfer in a liquid-fueled gas turbine combustor. The parametric studies examined the combustion characteristics, and spray flame struc-

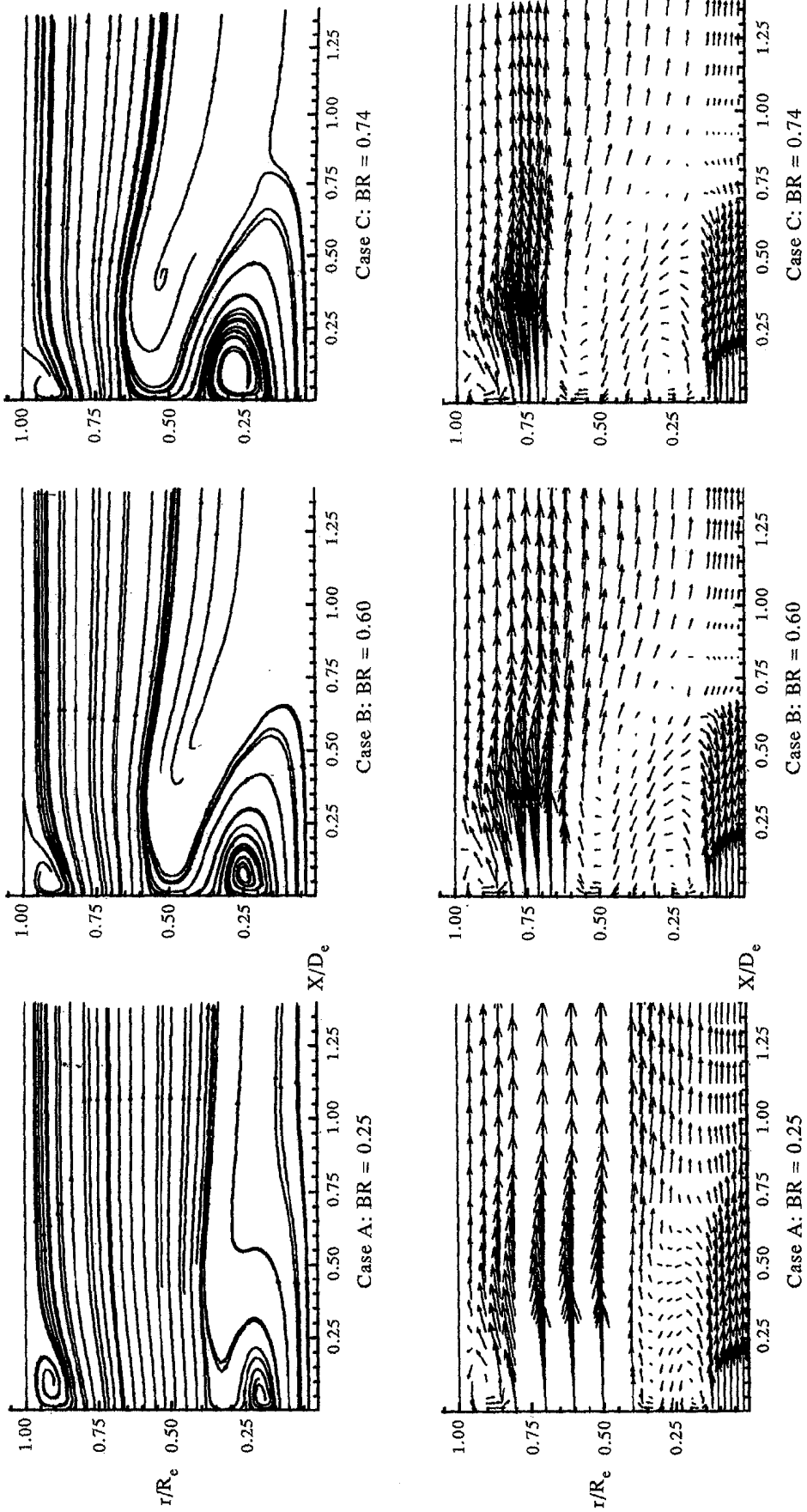


Fig. 2. Streamlines and axial velocity vectors for three different bluff-body ratios.

Table 1. Operation conditions

Case	A	B	C	D	E	F	G	H	
$d_1$ (mm)	8.05	8.05	8.05	8.05	8.05	8.05	8.05	8.05	
$d_2$ (mm)	25.2	38.8	43.2	38.8	38.8	38.8	38.8	38.8	
$d_s$ (mm)	50.25	50.25	50.25	50.25	50.25	50.25	50.25	50.25	
$\alpha$ ( $^\circ$ )	0	0	0	15	30	45	30	30	
$D_e$ (mm)	62.50	62.50	62.50	62.50	62.50	62.50	62.50	62.50	
BR	0.251	0.596	0.740	0.596	0.596	0.596	0.596	0.596	
ER	1.24	1.24	1.24	1.24	1.24	1.24	1.24	1.24	
$U_p$ ( $\text{m s}^{-1}$ )	10.0	10.0	10.0	14.0	14.0	14.0	14.0	25.0	
$U_s$ ( $\text{m s}^{-1}$ )	17.9	17.9	17.9	25.0	25.0	25.0	14.0	14.0	
$U_p/U_s$	0.56	0.56	0.56	0.56	0.56	0.56	1.0	1.79	
$Re_p$	$5.25 \times 10^3$	$5.25 \times 10^3$	$5.25 \times 10^3$	$7.35 \times 10^3$	$7.35 \times 10^3$	$7.35 \times 10^3$	$7.35 \times 10^3$	$7.35 \times 10^3$	$1.31 \times 10^4$
$Re_s$	$1.40 \times 10^4$	$6.40 \times 10^3$	$3.94 \times 10^3$	$8.95 \times 10^3$	$8.95 \times 10^3$	$8.95 \times 10^3$	$8.95 \times 10^3$	$8.95 \times 10^3$	$1.60 \times 10^4$

ture, and were compared with the measured results. Also, the influence of bluff-body size on the velocity, temperature, fuel/oxygen concentration, and droplet distribution profiles was studied in detail. In this study, the modified spray combustion code was used for predicting the operation cases shown in Table 1. The parametric studies included the influence of the jet-to-air ratio, bluff-body cone angle and blockage ratio on the flow field and temperature profiles. *n*-Octane ( $\text{C}_8\text{H}_{18}$ ) is chosen as the fuel for this study. To render complex phenomena manageable, the following assumptions are made in this study:

- (1) The spray process is quasi-steady.
- (2) A one-step chemical reaction is assumed.
- (3) The diffusion coefficients are the same for all species, and the Lewis number is unity.
- (4) Radiation heat transfer is not considered.
- (5) Ignition does not take place in the liquid phase.

## RESULTS AND DISCUSSION

The bluff-body combustor can be regarded as a combination of the central primary fuel jet and the surrounding secondary air jet. When the primary jet

emerges from the recirculation zone formed by the surrounding secondary jet, the central jet and the surrounding jet act on each other, which then leads to the emergence of an air-driven vortex and a fuel-driven vortex in the recirculation zone. The air-driven vortex is caused by the shear layer in the division of the air flow around the edge of the bluff body and the fuel-driven vortex is caused by the central fuel jet. These two vortices turn in opposite directions. Besides, both their positions and their structures change according to the changes in the momentum of the two jets. As a result, two stagnation points may appear on the symmetric axis at different times, respectively caused by the central fuel jet and the surrounding air jet. The length of the recirculation zone ( $L_{rz}$ ) is defined as the distance between the fuel nozzle and the back stagnation point.

### Effect of bluff-body blockage ratio

*The recirculation zone behind the bluff body.* Figure 2 reveals that the smaller the blockage ratio, the smaller the recirculation zone behind the bluff body near the nozzle, and the weaker the circulation. However, there are greater variations in the velocity gradients in the major mixing zone. On the other hand, though a greater blockage ratio creates a greater recirculation zone behind the bluff body, and a stronger circulation, there is less variation in the velocity gradient in the major mixing zone. These results are similar to those from an experiment by Wingfield [2], who found that the fastest mixing between the primary fuel jet and the secondary air jet occurred when the bluff-body thickness  $d_2/d_1$  was between 2 and 3. Two findings follow from the results. First, the greater the bluff-body blockage ratio, the greater the decline in the velocity, and the stronger the circulation in the recirculation zone. Second, the further away from the nozzle the lowest velocity point is, the greater is the recirculation zone. The size of the recirculation zone is the major factor affecting flame persistence and flame stability.

*The central axial velocity and temperature profiles.* Figure 3 shows that, when the jet-to-air velocity ratio

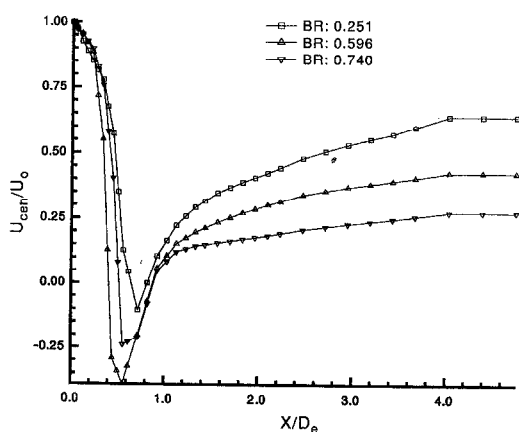


Fig. 3. Calculated axial velocity profiles along the centerline for three different bluff-body ratios.

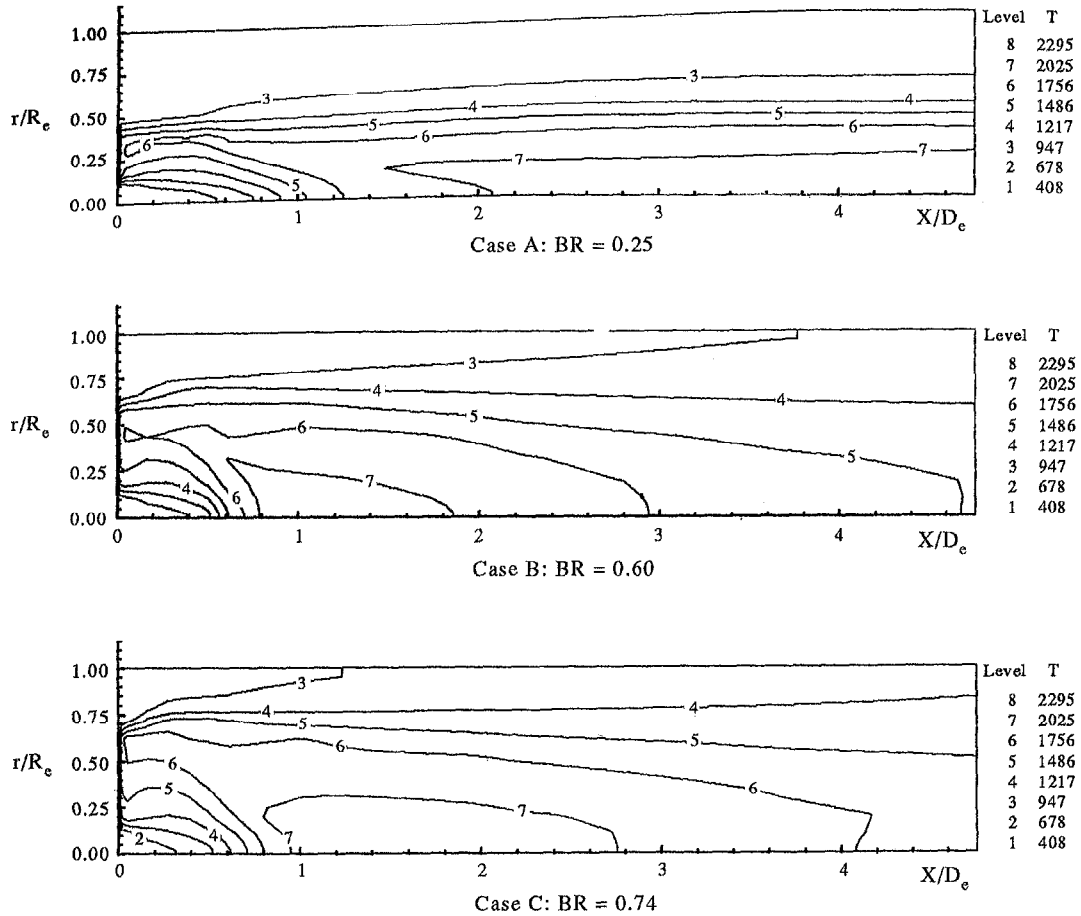


Fig. 4. Temperature contours for three different bluff-body ratios.

is smaller than 1.0 ( $U_p/U_s < 1.0$ ), the central axial velocity immediately decreases after leaving the nozzle, and then rises again to its highest point. This can be explained as follows. The secondary jet forms a recirculation zone behind the bluff body after passing it. When the primary jet is discharged from the recirculation zone, it has to overcome the incoming fluid. As a result, the central axial velocity tends to rapidly decrease after the primary jet leaves the nozzle. The greater the velocity of the incoming fluid, the greater the decline in the primary jet's velocity. The primary and secondary jets near the nozzle can be seen as two separate jets. After the primary jet leaves the recirculation zone, it combines with the secondary jet to form a single jet. Therefore, the center axial velocity of the primary jet tends to decline to the lowest point, and then rises to the highest point, which is the intermediate zone. In case A, the lowest velocity point is located near  $0.70D_e$ . In case C, the lowest velocity point is located near  $0.55D_e$ .

In case C, a stronger circulating vortex occurred in the wake of the larger bluff body. Thus, higher-temperature combustion products will penetrate into

the vortex and be carried upstream, where they may mix with fresh oxidizer. Figure 4 shows that chemical reactions take place earlier and the flame zone is located near the center line area for the larger bluff-body blockage ratio.

#### Effects of bluff-body cone angle

*The recirculation zone behind the bluff body.* Figure 5 shows the formation of the recirculation zone when the cone angle of the central bluff body changes. In case B, with a cylindrical bluff body (baseline case), the recirculation zone behind the bluff body is of moderate size, with limited turbulence, and interrupted presence. When the bluff-body cone angle increases to  $15^\circ$ , the recirculation zone behind the bluff body becomes larger and oval. When the angle increases continuously, the length of the recirculation zone shortens, but the width increases. As a result, the width of the recirculation zone increases, and the curvature increases, which leads to a slight shortening of the recirculation length. The length of the recirculation zone is around  $1.1\text{--}1.3d_2$ , and the width around  $1.1\text{--}1.2d_2$ . Pan *et al.* [8] measured the length

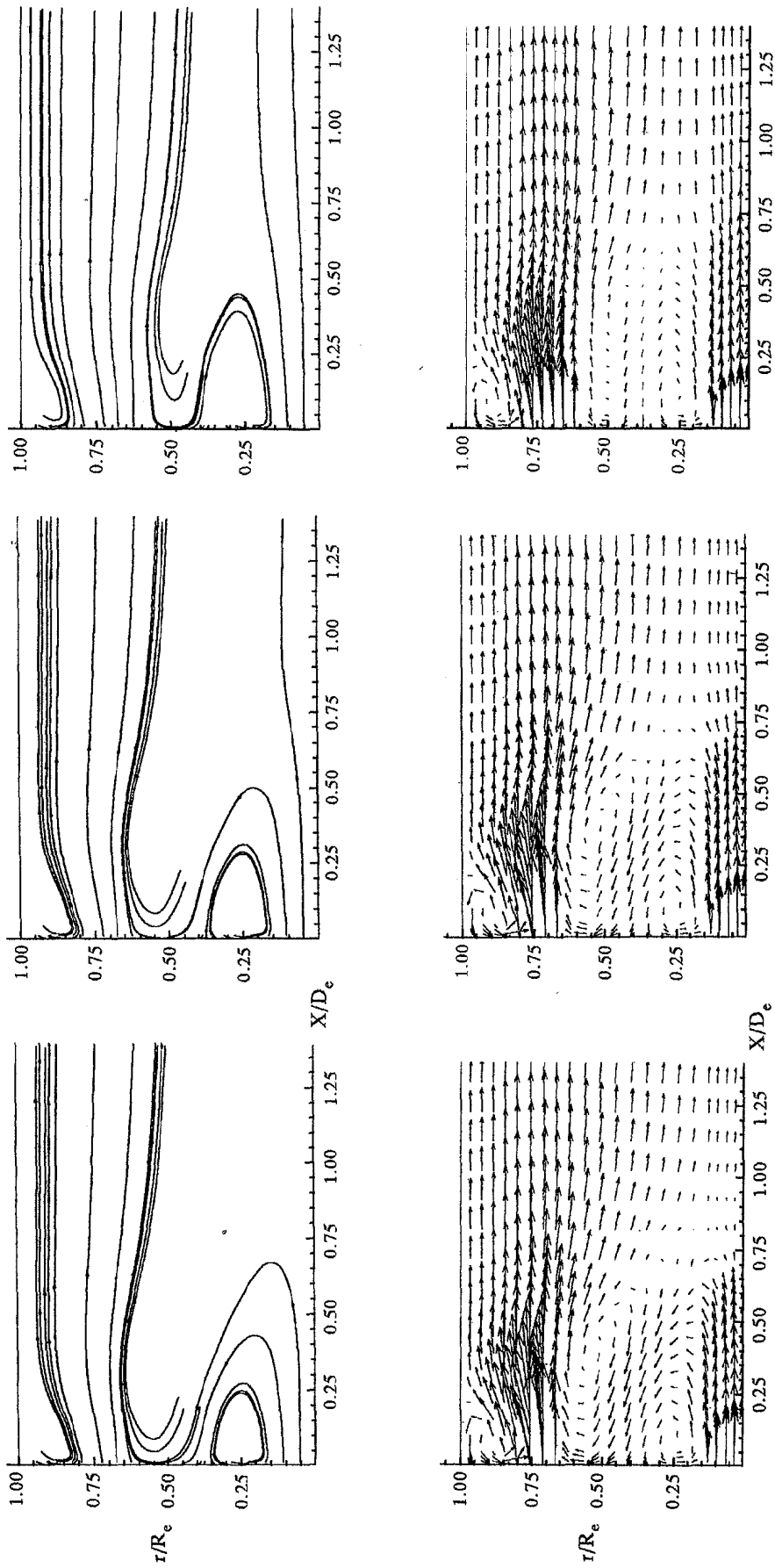


Fig. 5. Streamlines and axial velocity vectors for three different bluff-body cone angles.

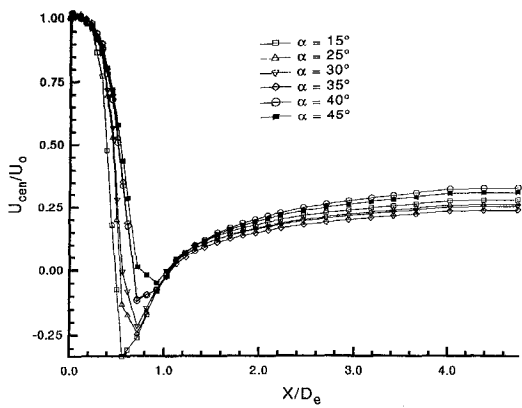


Fig. 6. Calculated axial velocity profiles along the centerline for different bluff-body cone angles.

of the recirculation zone of a cylindrical bluff body to be around  $1.5d_2$ , and the width to be around  $1.1d_2$ . They also noted that the recirculation zone consistently appeared behind the bluff body, and the primary jet caused considerable turbulence in it. This means that fuel would be absorbed in the recirculation zone at this time. Besides, a substantial amount of

turbulence represents a better mixture of fuel and air, which makes it easier to achieve a more stable flame.

*The central axial velocity and temperature profiles.* Figure 6 is a comparison of the distribution of the central axial velocity for different bluff-body cone angles. It shows that the lowest velocity point of case D ( $\alpha = 15^\circ$ ) is about  $0.6D_e$ . There are negative velocities on the central axis in all cases. Therefore, there are two stagnation points with zero velocity on the central axis. The front and back stagnation points are caused, respectively, by the central primary jet and the surrounding secondary jet. Part of the fluid in the secondary jet is absorbed back upstream at the back stagnation point. It slopes outward in a vertical direction after reaching the front stagnation point, and reacts with the fluid from the primary jet. This also demonstrates that an increase in the bluff-body cone angle leads to an increase in the intensity of the circulation in the recirculation zone behind the bluff body.

The calculated lengths of the recirculated zone are shorter when the bluff-body cone angle increases. Figure 7 shows that a slim and longer flame happened at cone angle  $\alpha = 15^\circ$ , and a denser and shorter flame happened at cone angle  $\alpha = 30^\circ$ . There is only a small temperature difference between  $\alpha = 30^\circ$  and  $\alpha = 45^\circ$ .

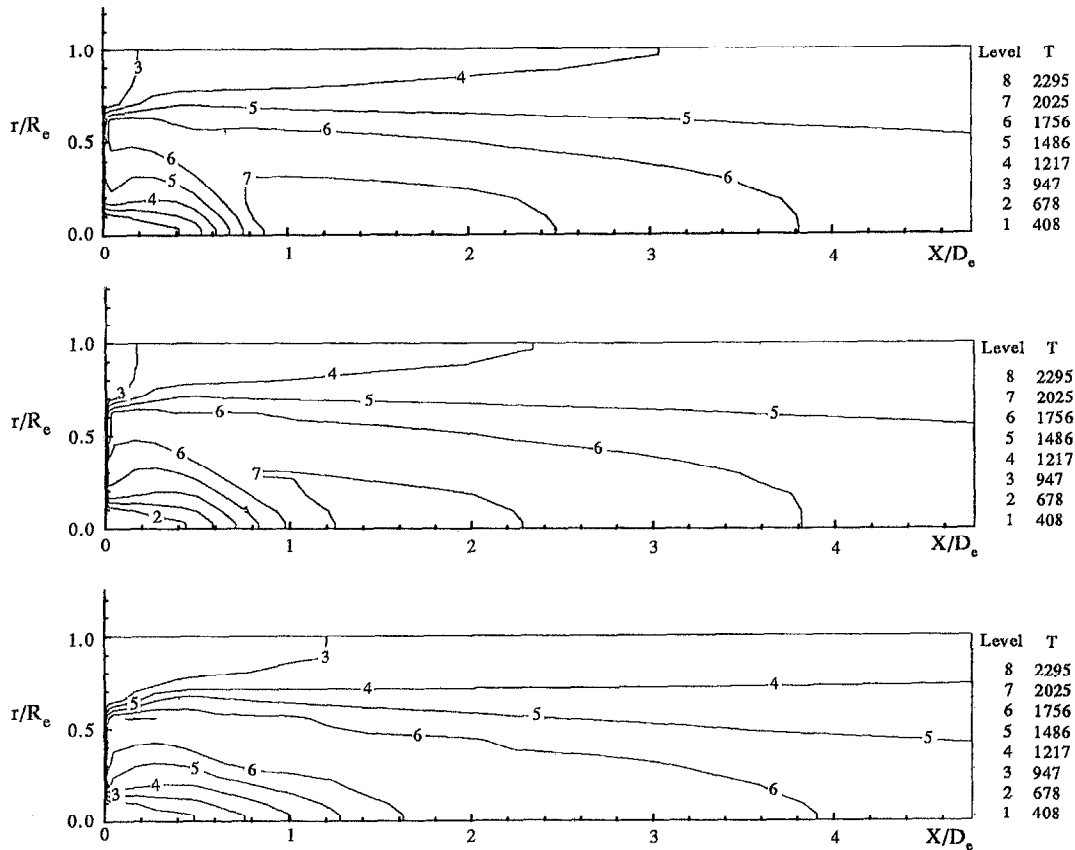


Fig. 7. Temperature contours for three different bluff-body cone angles.



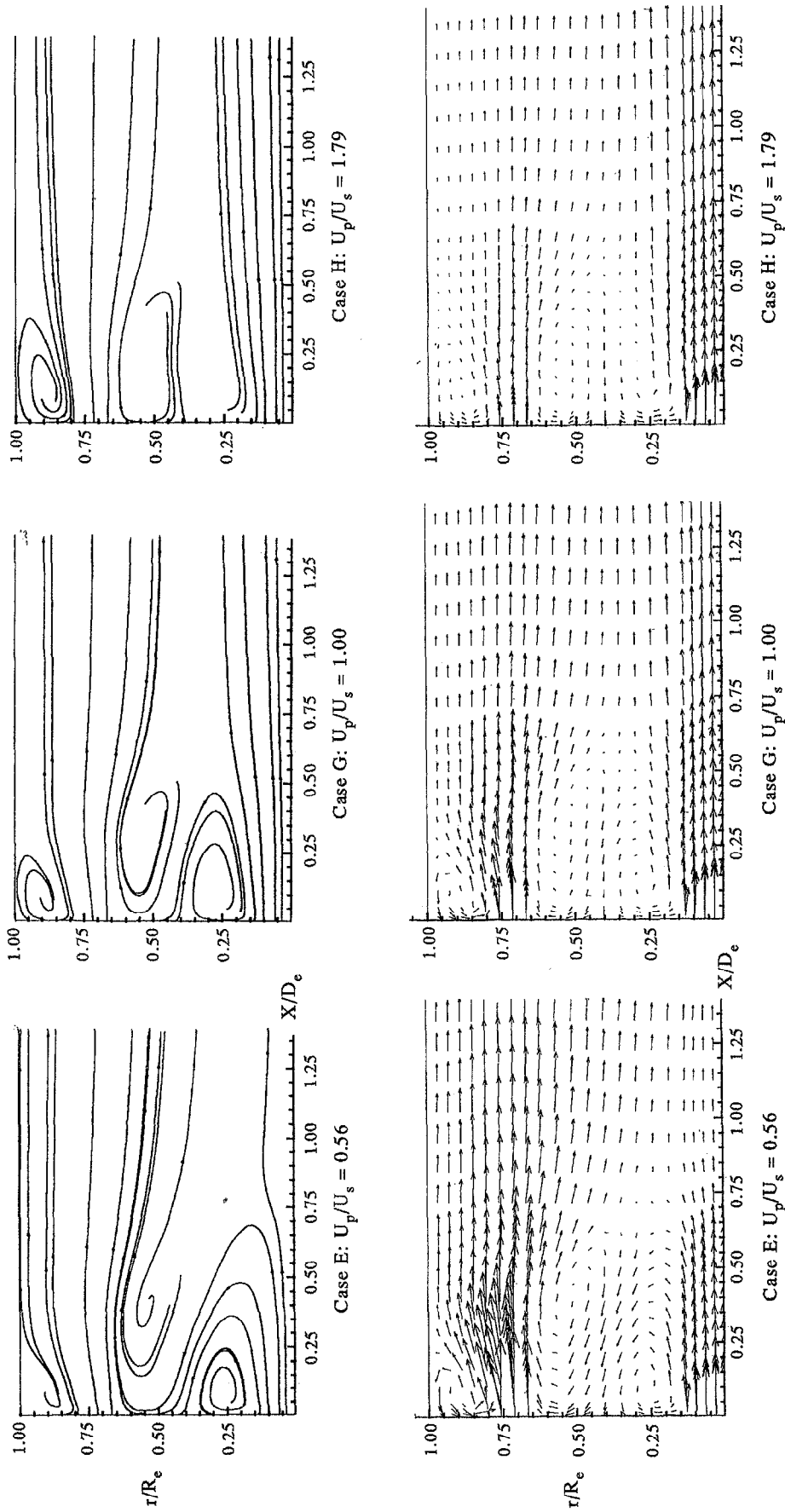


Fig. 8. Streamlines and axial velocity vectors for three different jet-to-air velocity ratios.

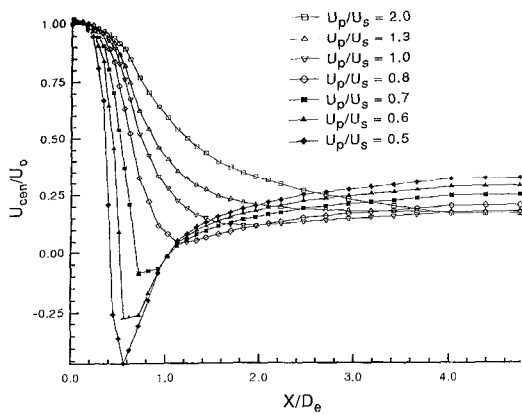


Fig. 9. Calculated axial velocity profiles along the centerline for different jet-to-air velocity ratios.

*Effects of jet-to-air velocity ratio ( $U_p/U_s$ )*

*The recirculation zone behind the bluff body.* Figure 8 shows streamlines and axial velocity vectors for different jet-to-air velocity ratios. In case E, with a jet-to-air velocity ratio of 0.56, the primary jet is thus brought upstream by the secondary jet. Therefore, the fuel from the primary jet is absorbed into the recirculation zone. In case G, with a velocity ratio of

1.0, a small portion of the primary jet is brought upstream, and the recirculation zone behind the bluff body thus appears weak. In case H, where the jet-to-air velocity ratio further increases to 1.79, the velocity of the primary jet is greater than that of the secondary jet. The fuel then turns into an arc and quickly slopes toward the center after leaving the nozzle. Therefore, the velocities of the primary and secondary jets have a considerable effect on the recirculation zone behind the bluff body. They determine whether the burning flame is controlled by the secondary air jet or the primary fuel jet. For a lower jet-to-air velocity ratio ( $< 1.0$ ), more fuel from the primary jet is carried into the recirculation zone behind the bluff body. A better mixing of fuel and air, enabling the flame to remain instead of being blown out, thus achieves a better flame persistence.

*The central axial velocity and temperature profiles.* As shown in Fig. 9 when the jet-to-air velocity ratio is smaller than 1.0, the central axial velocity of the primary jet immediately decreases after leaving the nozzle, then rises to the highest point, and finally gradually decreases. There will be two stagnation points with zero velocity on the central axis. When the jet-to-air velocity ratio is equal to or greater than 1.0, the fluid of the primary jet decreases after leaving the nozzle, without the phenomenon of a decline fol-

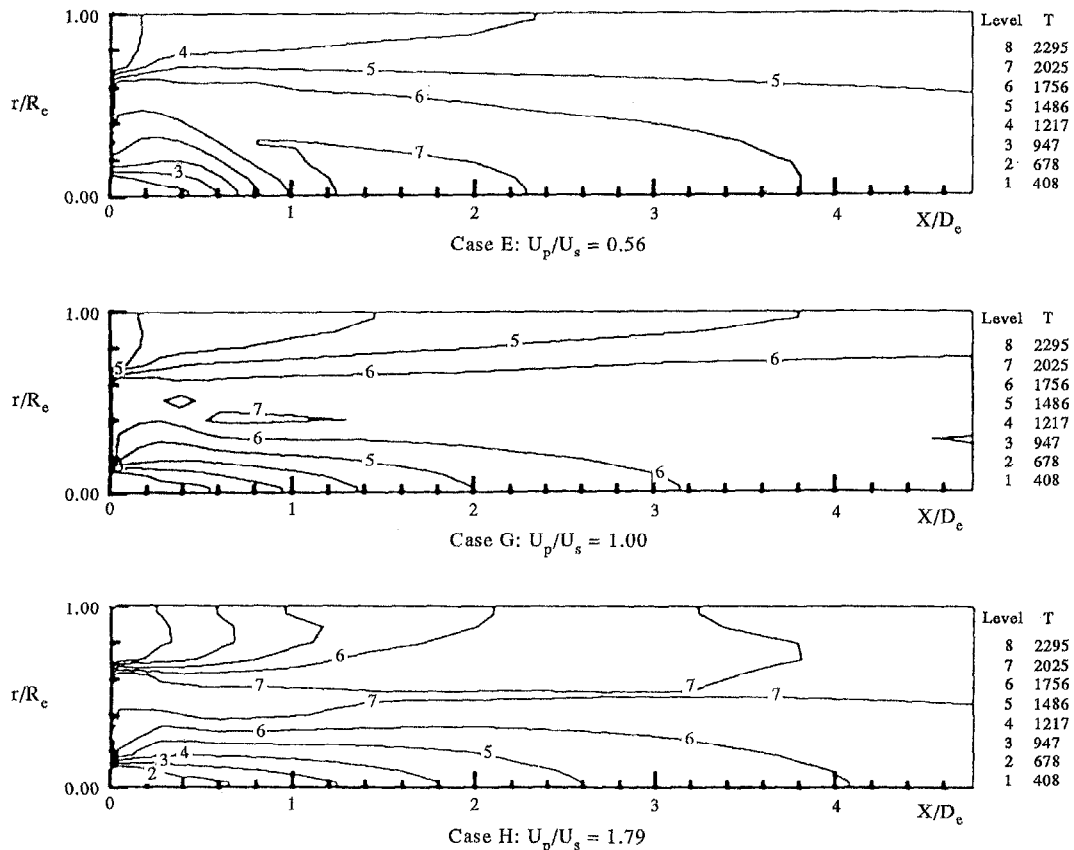


Fig. 10. Temperature contours for three different jet-to-air velocity ratios.

lowed by an increase. The reason is that the circulation force of the recirculation zone formed by the secondary jet is not strong enough to counter the fluid from the primary jet. From cases G and H, we found that all the areas with the greatest variation in velocity gradient fall between  $0.2$  and  $1.2D_e$ . The changes gradually slow down after that. In case E, there are larger average velocity gradients in the mixed areas.

A smaller jet-to-air velocity ratio ( $U_p/U_s < 1.0$ ) leads to a more intense turbulence in the recirculation zone formed behind the bluff body. A circulating fuel-driven vortex occurred in the wake of the bluff body. Higher-temperature combustion products will penetrate into the vortex and be carried upstream, where they may mix with fresh oxidizer. Thus, chemical reactions take place earlier and the flame zone is located near the combustor (cf. Fig. 10). This accounts for flame stabilization. On the contrary, at a greater jet-to-air velocity ratio ( $U_p/U_s > 1.0$ ), the fuel jet will penetrate the air-driven vortex with a longer flame.

### CONCLUSION

The following is a summary of the findings and conclusions.

(1) There are two large structural eddies in the recirculation zone behind the bluff body. The revolving directions of these two eddies happen to be opposite. The jet-to-air velocity ratio ( $U_p/U_s$ ) determines whether the circulation field is controlled by the primary or the secondary jets. If the secondary jet controls the circulation field ( $U_p/U_s < 1.0$ ), the fuel from the primary jet will be brought into the recirculation zone. On the contrary, if the primary jet controls the circulation field ( $U_p/U_s > 1.0$ ), only a little fuel from the primary jet could be absorbed into the recirculation zone.

(2) Two front and back stagnation points could be found along the central axis where  $U_p/U_s < 0.7$ . However, they will not be found when  $U_p/U_s > 1.0$ .

(3) The length of the recirculation zone behind the bluff body could be calculated based upon the front and back stagnation points. The length of the recir-

ulation zone for the reaction flow is in agreement with previous findings [12].

(4) Proper bluff-body blockage ratios, cone angles, and a smaller jet-to-air velocity ratio can lead to a more intense turbulence in the recirculation zone formed behind the bluff body. This means a better fuel air mixture, which makes it easier to achieve a better flame stability.

*Acknowledgement*—This research was funded by the National Science Council of the Republic of China (NSC 81-0401-E002-584).

### REFERENCE

1. A. B. Hedley and E. W. Jackson, Recirculation and its effects in combustion systems, *J. Inst. Fuel* **38**, 290–297 (1965).
2. G. J. Wingfield, Mixing and recirculation pattern from double concentric jet burners using an isothermal model, *J. Inst. Fuel* **40**, 456–464 (1967).
3. M. A. Habib and J. H. Whitelaw, Velocity characteristics of a confined coaxial jet, *J. Fluids Engng* **101**, 521–529 (1979).
4. G. D. Simth, T. V. Giel and C. G. Catalano, Measurements of reactive recirculating jet mixing in a combustor, *AIAA J.* **21**(2), 270–276 (1983).
5. R. W. Schefer, M. Namazian and J. Kelly, Velocity measurements in a turbulent nonpremixed bluff-body stabilized flame, *Combust. Sci. Technol.* **56**, 101–138 (1987).
6. R. H. Chen, J. F. Driscoll, J. Kelly, M. Namazian and R. W. Schefer, A comparison of bluff-body and swirl stabilized flames, *Combust. Sci. Technol.* **71**, 197–217 (1990).
7. J. C. Pan, M. D. Vangsness and D. R. Ballal, Aerodynamics of bluff-body stabilized confined turbulent premixed flames, *J. Engng Gas Turbines Power* **114**, 783–789 (1992).
8. J. C. Pan, W. J. Schmoll and D. R. Ballal, Turbulent combustion properties behind a confined conical stabilizer, *J. Engng Gas Turbines Power* **114**, 33–38 (1992).
9. M. Namazian, J. Kelly and R. W. Schefer, Concentration imaging measurements in turbulent concentric-jet flows, *AIAA J.* **30**(2), 384–394 (1992).
10. L. F. Martins and A. F. Ghoniem, Simulation of the nonreacting flow in a bluff-body burner; effect of the diameter ratio, *Trans. ASME* **115**, 474–484 (1993).
11. H. K. Ma, M. Y. Wang and F. H. Lee, The study of spray combustion characteristics in a bluff-body combustor, *J. Chin. Soc. Mech. Engrs* **14**(1), 10–25 (1993).
12. H. K. Ma, F. H. Lee and M. Y. Wang, Numerical study on heat and mass transfer in a liquid-fueled gas turbine combustor, *Int. J. Heat Mass Transfer* **36**, 3271–3281 (1993).